A novel scheme of cascaded four-wave mixing for phase-sensitive amplification in nonlinear optical fibre

Abhishek Anchala, Pradeep Kumar Krishnamurthyb and Pascal Landaisc

Department of Applied Physics, The Rachel and Selim Benin School of Computer Science and Engineering, The Hebrew University of Jerusalem, Jerusalem, Israel;

Department of Electrical Engineering, Indian Institute of Technology Kanpur, Kanpur, India;

School of Electronic Engineering, Dublin City University, Dublin, Ireland

ABSTRACT

We propose and numerically verify a scheme of phase-sensitive amplifier (PSA) using four-wave mixing (FWM) in cascaded highly nonlinear fibres (HNLFs), without requiring initial phase-locking between signal and pump. The first HNLF is used to generate two phase-conjugate waves, which act as two pumps for FWM process in second HNLF. We feed the two pumps from opposite ends of second HNLF and a signal co-propagating with one of the pumps. We keep the signal frequency in the middle of two pump frequencies to obtain phase-conjugate wave at the same frequency as the signal by FWM process in second HNLF. Signal and phase-conjugate wave appear at opposite ends of the second HNLF and combined to obtain PSA. The frequency-shift-free operation of phase conjugation helps in preserving the frequency of input signal during phase-sensitive amplification. We derive the expression for PSA signal output and PSA gain and show analytically that PSA gain depends upon signal phase only, as the two pumps are phase conjugate to each other. Thus, eliminating the need of phase locking between signal and pump waves. We show that PSA provides high gain for in-phase component and almost cancellation for quadrature-phase component of signal. We show the broadband nature of PSA due to minimum effect of group velocity and group velocity dispersion owing to counter-propagating nature of signal and conjugate waves. We study the performance of PSA under the effects of pump-signal detuning, amplifier length and input signal phase. Simulation results show that PSA output is forced to attain 0 or π phase regardless of large variation of phase in the input signal. Nonlinear phase noise reduction of 100 Gbps DPSK signal transmitted over 1000-km standard single-mode fibre confirms phase regeneration by PSA.

1. Introduction

Phase-sensitive amplifiers (PSAs) have been studied extensively in recent years as they play a key role in all-optical signal processing including phase regeneration and signal sampling. This is due to its ability to provide gain that depends on the phase of input signal relative to local optical reference (*1–3*). Particularly, PSA's capability to squeeze the noise below the quantum limit in one of the two phase quadrature is useful in phase re-generation of phase-shift keying (PSK) signals, resulting in suppression of frequency and timing jitter (*4*, *5*). PSA also provides amplification without adding excess spontaneous emission noise having 0 dB noise figure (NF) in contrast to 3 dB quantum limit in phase-insensitive amplifiers (PIAs) such as erbium-doped fibre amplifiers (*6*). The phase-dependent gain and noiseless amplification of PSA is very attractive for nonlinear phase noise reduction (Gordon–Mollenauer phase noise), phase re-generation, low-noise amplification, format conversion of phase-encoded signals and improvement of optical signal-to-noise ratio (*7–9*). PSA has also been used in sensitivity improvement and enhancement of transmission distance in a multi-span fibre link by replacing PIAs with PSAs (*10*, *11*).

PSAs have been demonstrated in materials with second-order nonlinearity in periodically poled Lithium Niobate and with third-order nonlinearity in a highly nonlinear fibre (HNLF), semiconductor optical amplifiers and silicon and chalcogenide waveguide (*2*, *3*, *12–16*). Among these media, realization of PSA in HNLF is notably interesting for practical network applications due to its low loss, long interaction length for nonlinear amplification, high-power efficiency and ease of system integration (*6*, *7*, *17–19*). Two techniques of PSA based on HNLF have been demonstrated: nonlinear optical loop mirror (NOLM) and phase-sensitive fibre optical parametric amplifier (FOPA) (*4*, *9*, *17–20*). In NOLM based PSA, signal and pump (optical reference at signal frequency) waves are used at same frequency, leading to degradation in signal quality due to guided acoustic-wave Brillouin scattering of pump waves (*20*, *21*). Hence, research efforts have been shifted to PSA based on phase-sensitive FOPA. PS-FOPA can be realized in frequency nondegenerate and frequency degenerate manners. In frequency nondegenerate PS-FOPA, signal and idler are in different frequencies resulting in shift of operating frequency at PSA output, which may lead to cross-talk when applied in WDM systems (*18*, *19*). More-over, pump waves are also present at the output of PSA, in addition to amplified signal, which acts as classical noise source. In frequency degenerate, PS-FOPA signal and idler are present at the same frequency, hence there is no shift in operating frequency (*4*, *22*, *23*). However, in this technique, an optical phase locking between signal and pump waves is required.

In this paper, we propose and numerically verify a new technique to realize frequency degenerate PSA without requiring phase locking between signal and pump waves using cascaded four-wave mixing in two HNLFs. The FWM process is established in a first HNLF stage to generate two phase-conjugated waves, which act as pumps for the second FWM process in the second HNLF. The two phase-conjugated pump waves are input to opposite ends of the second HNLF along with the co-propagating signal wave with one of the pump waves, to realize frequency-shift-free optical phase conjugation (FS-OPC), as reported in our previous work (*24*, *25*). By keeping the signal frequency in the middle of two pump frequencies, the generated conjugate wave has the same frequency as that of the signal. The conjugate and signal waves appear at the opposite ends of the second HNLF and an optical filter is used to remove the pump waves. The filtered signal and conjugate waves are combined to generate PSA. The generation of conjugated wave at the signal frequency avoids the frequency conversion of signal at PSA output, whereas the absence of pump waves at PSA output reduces the possibility of adding noise and improves the noise figure of PSA.

We investigate the phase-dependent gain of proposed PSA analytically and show that PSA gain depends upon signal phase only, as the average phase of two phase-conjugate pump waves is zero, thus eliminating the need of phase locking between signal and pump waves. We further show analytically that PSA provides high gain for in-phase and loss for quadrature phase of signal, resulting in high gain extinction ratio (GER) (~ 25 dB). We show analytically that effects of group velocity and group velocity dispersion are minimized due to counter-propagating nature of signal and conjugate waves, resulting in large bandwidth of our proposed PSA. We investigate the performance of proposed PSA by simulating the dependence of phase and power of signal at PSA output on HNLF length, input signal power and input signal phase. The prediction derived from analytical expression shows excellent agreement with numerical simulation. Finally, using numerical simulations, we show the phase regeneration of 100 Gbps differential phase-shift keying (DPSK) signal transmitted over 1000-km standard single-mode fibre (SSMF) link.

The advantages of our proposed PSA are (a) *no requirement of phase locking between signal and pump waves*,

(b) no shift in operating frequency, (c) *absence of pump waves at PSA output* and (d) *high GER*. The paper is organized as follows: In Section 2, we briefly discuss the theory and analytical description of PSA using cascaded FWM in two HNLF. In Section 3, we present the simulation results of our proposed scheme of PSA. In Section 4, we verify the phase-regenerative property of the proposed PSA for DPSK transmission. Finally, we conclude by summarizing our results in Section 5.

2. System description

Figure 1 shows the schematic diagram of the proposed method to generate PSA using cascaded FWM in two HNLF. In HNLF1, amplified signal wave at frequency ω_S interacts with pump1 at frequency ω_1 via FWM to generate pump2 at frequency ω_2, such that two pumps are phase conjugate to each other. The frequency assignment of signal and pump waves are shown in Figure 1, where

is detuning between signal and pump waves. The two phase-conjugate pumps are input into opposite ends of HNLF2 along with a signal co-propagating with pump1 to generate FS-OPC, as shown in the dotted box of Figure 1. In HNLF2, two pumps and signal create two Bragg grat-ings: grating1 due to interaction between pump1 and signal and grating2 due to interaction between pump2 and signal. A backward travelling conjugate wave (relative to signal) is generated by diffraction of pump2 and pump1 from grating1 and grating2, respectively. The symmetric placement of pump frequencies around the signal frequency results in conjugate wave at signal frequency i.e. at ω_S (*24–26*). An optical filter removes pump waves and the signal and conjugate waves are combined to observe constructive or destructive interference, depending on the input signal phase, thus obtaining phase-sensitive output at PSA. However, it is important to note that in order to create interference between signal and conjugate waves, a low-speed phase dithering associated with a feedback control loop is required to reduce the low-frequency thermal drift between the signal and conjugate path (not shown in Figure 1), as reported in our previous work (*27*). In Figure 1, EDFA is used to compensate the 3 dB signal loss at input coupler and band-pass filter is used to remove out of band amplified spontaneous emission (ASE) noise.

2.1. Mathematical analysis

The expression for PSA output can be obtained by solving the nonlinear Schrödinger equation (NLSE) in the two HNLFs,

$$\frac{\partial E}{\partial z} = -k^{(1)}\frac{\partial E}{\partial t} + j\frac{k^{(2)}}{2}\frac{\partial^2 E}{\partial t^2} - j\gamma|E|^2E, \qquad (1)$$

where E is the total electric field and γ is the nonlinear coefficient of the fibre (*28*).

2.1.1. Solving FWM in HNLF$_1$

Assuming, electric field of the two pumps and signal waves are given by $E_1(z, t) = A_1 \exp(j(\omega_1 t - k_1 z))$, $E_2(z, t) = A_2 \exp(j(\omega_2 t - k_2 z))$ and $E_S(z, t) = A_S \exp(j(\omega_S t - k_S z))$, respectively, where A_1, A_2, and A_S are slow varying pulse envelopes. Assuming strong pump approximation and that all waves are co-polarized, equations governing the evolution of pump1 and pump2 in HNLF1 can be obtained by substituting $E(z, t) = E_1(z, t) + E_2(z, t) + E_S(z, t)$ into (1), and simplifying we obtain,

$$\frac{\partial A_{1,2}(z,t)}{\partial z} = -\frac{\alpha}{2}A_{1,2} + j\gamma\left(|A_{1,2}|^2 + 2|A_{2,1}|^2 + 2|A_S|^2\right)A_{1,2} + 2j\gamma A_S^2 A_{2,1}^* e^{-j\Delta K_1 z}, \quad (2)$$

where $K_1 = 2k_S - k_1 - k_2$ and α is fibre attenuation. In (2), the first and second term accounts for attenuation and self-phase modulation (SPM) & cross-phase modu-lation (XPM) respectively, and fourth term accounts for FWM. Solving (2) by neglecting attenuation, SPM and XPM effects we obtain,

$$A_1(z) = \exp(-j\Delta K_1 z/2) \times \left[\cos(\mu_1 z) + \left(\frac{j\Delta K_1}{2\mu_1}\right)\sin(\mu_1 z)\right] A_{10}$$

$$A_2(z) = \frac{j\kappa_1}{2\mu_1}\exp(-j\Delta K_1 z/2)\sin(\mu_1 z)A_{10}^*, \qquad (3)$$

Where $\mu_1 = \sqrt{(\Delta K_1)^2 - 4|\kappa_1|^2}$, $\kappa_1 = 2\gamma A_{S0}^2$ and A_{10} is pump amplitude at z=0. Since the two pumps are obtained at $z = L_1$ of HNLF$_1$, the phase relation between at $z = L_1$ of HNLF$_1$, the phase relation between two pumps can be written as

$$\phi_1 = \theta_1 - \frac{\Delta K_1 L_1}{2} + \phi_{P_{10}}$$

$$\phi_2 = \frac{\pi}{2} - \frac{\Delta K_1 L_1}{2} + \phi_{P_{10}}^*, \qquad (4)$$

Where $\theta_1 = \tan^{-1}\left(\frac{\Delta K_1}{2\mu_1}\tan(\mu_1 L_1)\right)$

And $\phi_{P_{10}}$ is the pump 1 phase at z=0. Fro (4) we infer that pump 1 and pump 2 are phase conjugate to each other with additional phase $\Delta\phi = \theta_1 + \frac{\pi}{2} - \Delta K_1 L_1$ present.

2.1.2. Solving FWM in HNLF$_2$

The equations governing the signal and conjugate waves propagation in HNLF2 can be obtained by substituting total electric field $E(z, t) = A_1(L_1)\exp(j(\omega_1 t - k_1 z) + A_2(L_1)\exp(j(\omega_2 t + k_2 z) + A_S\exp(j(\omega_S t - k_S z)) + A_C\exp(j(\omega_S t + k_S z))$ into (1), and taking nearly phase-matched terms (*24*),

$$\frac{\partial A_{S,C}(z,t)}{\partial z} = \mp\frac{\alpha}{2}A_{S,C} + j\gamma\left(|A_{S,C}^2| + 2|A_{C,S}^2|\right)A_{S,C} + 2j\gamma\sum_{p=1,2}|A_p^2|A_{S,C} \pm 2j\gamma A_1(L_1) \times A_2(L_1)A_{C,S}^* e^{-j\Delta K_2 z}, \qquad (5)$$

where A_C is conjugate envelope, $K_2 = k_1 - k_2$ and α is fibre attenuation. In (5), the first, second and third term accounts for attenuation, self-phase modulation (SPM) and cross-phase modulation (XPM) respectively, and fourth term accounts for FWM.

Analytical solution of (5) is complex and to simplify the solution we neglect the attenuation, SPM and XPM in a first instance. Solving (5) subject to boundary conditions, $A_S(0) = A_{S0}$ and $A_C(L_2) = 0$, we obtain

$$A_S(z) = \frac{1}{\zeta}\exp(-j\Delta K_2 z/2)[\{\mu_2\cos(\mu_2(z-L_2)) + (j\Delta k_2/2)\sin(\mu_2(z-L_2))\}]A_{S0}$$
$$A_C(z) = -\frac{j}{\zeta^*}\kappa_2^*\sin(\mu_2(z-L_2))\exp(-j\Delta K_2 z/2)A_{S0}^*, \quad (6)$$

where L_2 = length of HNLF$_2$, $\zeta = \mu_2\cos(\mu_2 L_2) - j(\Delta K_2/2)\sin(\mu_2 L_2)$, $\mu_2 = \sqrt{|\kappa_2|^2 + (\Delta K_2/2)^2}$, $\kappa_2 = 2\gamma A_1^*(L_1)A_2^*(L_1)$, $A_{S0} = \frac{GA_{sig}}{\sqrt{2}}$, G = EDFA gain, and

A_{sig} = input signal amplitude. Expression for PSA output is obtained by combining signal and conjugate wave at the opposite end of HNLF after filtering the pump$_2$ and pump$_1$ waves, respectively, i.e. $A_S(L_2)$ and $A_C(0)$:

$$A_{PSA} = \frac{\mu_2 e^{-j\Delta K_2 L_2/2}}{\zeta}A_{S0} + \frac{j\kappa_2^*\sin(\mu_2 L_2)}{\zeta^*}A_{S0}^*. \quad (7)$$

From (7), signal power at PSA output is

$$P_{PSA} = |A_{PSA}|^2 = \frac{P_{S0}}{|\zeta|^2}[\mu_2^2 + 4\gamma^2 P_1 P_2\sin^2(\mu_2 L_2) + 4\mu_2\gamma\sqrt{P_1 P_2}\sin(\mu_2 L_2)\cos(\theta_2 - 2\phi_{rel})], \quad (8)$$

where $\theta_2 = \frac{\pi}{2} + \frac{\Delta K_2 L_2}{2} - 2\tan^{-1}\left(\frac{\Delta K_2}{2\mu_2}\tan(\mu_2 L_2)\right)$, $\phi_{rel} = \phi_S - \frac{\phi_1+\phi_2}{2}$

is relative phase between signal phase and average of two pump phase at input of HNLF$_2$, and P_1, P_2 and P_{S0} are powers of pump$_1$, pump$_2$ and signal, respectively, at input of HNLF$_2$. Substituting the value of φ_1 and φ_2 from (4) in φ_{rel} , we obtain,

$$\phi_{rel} = \phi_S - \frac{1}{2}\left(\frac{\pi}{2} + \theta_1 - \Delta K_1 L_1\right). \quad (9)$$

The relative phase φ_{rel} depends upon signal phase only, and hence, the signal power gain of PSA, defined as $G = \frac{P_{PSA}}{P_{S0}}$, becomes,

$$G = \frac{1}{|\zeta|^2}[\mu_2^2 + 4\gamma^2 P_1 P_2\sin^2(\mu_2 L_2) + 4\mu_2\gamma\sqrt{P_1 P_2}\sin(\mu_2 L_2)\cos(2\phi_S - \theta)] \quad (10)$$

where $\theta = \theta_1 + \theta_2 - K_1 L_1$. Thus, the PSA gain G de-pends upon signal phase only and hence two pumps and input signal need not be synchronized by phase locking, which is otherwise a difficult process to achieve in optical domain (*22*, *29*). It is also observed that PSA gain depends upon amplifier length (HNLF$_2$ length), nonlinear co-efficient (γ) and pump powers. The PSA gain can be maximum or minimum depending upon $2\varphi_S - \theta = 0$ or π.

$$G_{max,min} = \frac{1}{|\zeta|^2}\left[\mu_2 \pm 2\gamma\sqrt{P_1 P_2}\sin(\mu_2 L_2)\right]^2, \quad (11)$$

where + and − signs go for maximum and minimum gain, respectively.

2.1.3. Gain extinction ratio

The GER defines the ability of PSA to amplify or deam-plify signal at selective signal phase (*18*). Mathematically, GER is defined as

$$\mathrm{GER} = \frac{G_{max}}{G_{min}} = \left[\frac{\mu_2 + 2\gamma\sqrt{P_1P_2}\sin(\mu_2 L_2)}{\mu_2 - 2\gamma\sqrt{P_1P_2}\sin(\mu_2 L_2)}\right]^2. \quad (12)$$

At optimum amplifier length (L_2 or $L_{op} = 2^{\pi}\mu_2$) (*24*) and for low pump powers, $\theta \approx 0$ and PSA gain (10) can be written as,

$$G = \frac{1}{|\zeta|^2}\left[\mu_2^2 + 4\gamma^2 P_1P_2 + 4\mu_2\gamma\sqrt{P_1P_2}\cos(2\phi_S)\right]. \quad (13)$$

From (13), we see that G is maximum for φS = 0 or π and is minimum for π/2. This phase-dependent gain by PSA forces the output signal to attain only 0 or π phase for large variation of input signal phase. It is important to note that due to low pump powers FWM efficiency in HNLF2 is low and hence we get low PSA gain G; however, due to high GER, PSA can perform better selectivity of signal phase and can be used in regeneration of phase-degraded PSK signals.

The above formulations are valid for the pulse propagation in PSA, as we keep the all interacting waves near zero-dispersion wavelength (ZDW ~ 1540 nm) of HNLF at which dispersion length is very high for HNLF with small dispersion parameter (D = 0.4 ps/nm km) (*24*, *30*). We also neglected the stimulated Brillouin effect (SBS) and stimulated Raman effect (SRS) in HNLF, while the former can be suppressed by the use of straining or Al-doped HNLF with increased SBS threshold (*31*, *32*), the latter has proven to substantially enhance the PSA gain (*33*). Further, the effect of SBS and SRS can be minimized by choosing detuning between signal and pump waves away from gain spectrum of SBS and SRS (*28*).

2.1.4. Effect of detuning and dispersion

When detuning between signal and pump waves ( ) is increased the signal or pump waves are no longer near ZDW of HNLF2; the effect of dispersion on signal and conjugate wave propagation and thus on PSA gain can be obtained by considering the pulse envelope of signal and conjugate wave i.e. $E_S(z, t) = A_S(t) \exp(j(\omega_S t - k_S z))$ and $E_C(z, t) = A_C(t) \exp(j(\omega_S t + k_S z))$, respectively. Solving (1) with $E(z, t) = A_1(L_1) \exp(j(\omega_1 t - k_1 z)) + A_2(L1) \exp(j(\omega_2 t + k_2 z)) + E_S(z, t) + E_C(z, t)$ and keeping only those term satisfying energy conservation and having minimum phase mismatch, we obtain the expression for signal and conjugate wave propagation after rearranging the terms as,

$$\begin{aligned}\frac{\partial A_{S,C}(z,t)}{\partial z} &= \mp\frac{\alpha}{2}A_{S,C}(t) \pm 2j\gamma A_1(L_1) \\ &\times A_2(L_1)A^*_{C,S}e^{-j\Delta K_2 z} - \frac{jk^{(2)}}{2}\frac{\partial^2 A_{S,C}(t)}{\partial t^2} \\ &+ \left[k^{(2)}\omega_S - k^{(1)}\right]\frac{\partial A_{S,C}(t)}{\partial t} \\ &+ j\left[\frac{k^{(2)}\omega_S^2}{2} - k^{(1)}\omega_S\right]A_{S,C}(t). \quad (14)\end{aligned}$$

Taking Fourier transform on (14) and rearranging the terms,

$$\frac{\partial \tilde{A_{S,C}}}{\partial z} = \pm 2j\gamma A_1(L_1)A_2(L_1)\tilde{A_{C,S}}^* e^{-j\Delta K_2 z} - \left[\mp\frac{\alpha}{2} + j\left\{k^{(1)}\Omega - k^{(2)}\omega_S\Omega - \frac{k^{(2)}(\Omega^2+\omega_S^2)}{2}\right\}\right]\tilde{A_{S,C}}. \quad (15)$$

Taking Fourier transform on (14) and rearranging the terms,

$$\frac{\partial \tilde{A_S}}{\partial z} = 2j\gamma A_1(L_1)A_2(L_1)\tilde{A_C}^* e^{-j\Delta kz} - E\tilde{A_S}$$
$$\frac{\partial \tilde{A_C}}{\partial z} = -2j\gamma A_1(L_1)A_2(L_1)\tilde{A_S}^* e^{-j\Delta K_2 z} - F\tilde{A_C}, \quad (16)$$

where $E = \left[\frac{\alpha}{2} + j\left\{k^{(1)}\Omega - k^{(2)}\omega_S\Omega - \frac{k^{(2)}(\Omega^2+\omega_S^2)}{2}\right\}\right]$ and
$F = \left[-\frac{\alpha}{2} + j\left\{k^{(1)}\Omega - k^{(2)}\omega_S\Omega - \frac{k^{(2)}(\Omega^2+\omega_S^2)}{2}\right\}\right]$.

We obsserve that E and F are complex constant containing attenuation, group velocity and GVD and satisfying

$$E + F^* = 0. \quad (17)$$

Performing the transformation $\widetilde{A_s} = \widetilde{B_s}\exp(-Ez)$ and $\widetilde{A_c} = \widetilde{B_c}\exp(-Fz)$ in (16), we obtain

$$\frac{\partial \tilde{B_S}}{\partial z} = 2j\gamma A_1(L_1)A_2(L_1)\tilde{B_C}^* e^{-j\Delta K_2 z} e^{(E+F^*)z},$$
$$\frac{\partial \tilde{B_C}}{\partial z} = -2j\gamma A_1(L_1)A_2(L_1)\tilde{B_S}^* e^{-j\Delta K_2 z} e^{(E^*+F)z}. \quad (18)$$

From (17), (18) is reduced to

$$\frac{\partial \tilde{B_S}}{\partial z} = 2j\gamma A_1(L_1)A_2(L_1)\tilde{B_C}^* e^{-j\Delta K_2 z},$$
$$\frac{\partial \tilde{B_C}}{\partial z} = -2j\gamma A_1(L_1)A_2(L_1)\tilde{B_S}^* e^{-j\Delta K_2 z}. \quad (19)$$

A comparison between (19) and (5) neglecting attenu-ation, SPM and XPM effects shows that the effects of $k^{(1)}$ and $k^{(2)}$ cancel and residual phase mismatch (K_2) remains the same owing to counter propagation of signal and conjugate waves. Hence, the group velocity and GVD have minimum or no effect on propagation of signal and conjugate pulses in our PSA scheme. Thus, at large detuning (Ω), high FWM efficiency in HNLF2 can be obtained, causing fairly constant PSA gain at large signal bandwidth.

3. Simulation results

In this Section, we investigate the performance of our proposed PSA by evaluating the theoretical expressions (7)–(13) and simulating (5) for variation in amplifier length (HNLF2 length) and signal phase, neglecting the contribution of attenuation (α = 0), SPM and XPM effects in HNLF. We verify

that the simulation results are in close agreement with theoretical values. Later, we account for the effects of SPM and XPM with $\alpha = 0.9$ dB km^{-1} into simulation and compare with former results. The HNLF parameters are zero dispersion wavelength (ZDW) at 1540 nm, $\alpha = 0.9$ dB km^{-1}, and $\gamma = 9.3$ /W/km for commercially available fibre (30). EDFA gain and noise figure are kept at 3 and 5 dB, respectively. Wavelength of $pump_1$, $pump_2$ and signal waves are taken as 1539.5, 1540.5 and 1540 nm, respectively. Detuning ($\Omega/2\pi$) is kept at 63.25 GHz to minimize the effect of SBS and SRS, as discussed in Section 2. The signal power is kept at −4 dBm. Linewidth of signal and pump waves are taken as 100 and 10 kHz, respectively, whereas OSNR of signal and pump waves is kept at 40 and 60 dB, respectively.

3.1. PSA output power vs. amplifier length

We studied the effect of variation of amplifier length ($HNLF_2$ length) from $0.1L_{op}$ to $2L_{op}$ on PSA output power. Figure 2 shows the output power of PSA in the case of $\varphi_S = 0$ plotted as a function of amplifier length for $\alpha = 0$ and $\alpha = 0.9$ dBkm^{-1} without and with SPM and XPM effects. The signal power increases with amplifier length and a peak power of −1.49 dBm is obtained at optimum length L_{op} for $\alpha = 0$; however, beyond L_{op} signal power decreases. This is because zero phase offset is present at amplifier length of L_{op}, causing an efficient FWM process and hence phase conjugation (*24*). The simulation results match closely with the theoretical value. When the effects of attenuation $\alpha = 0.9$ dB/km, SPM and XPM are taken into account, the PSA output power decreases significantly due to attenuation of signal and pump waves, as well as the inclusion of SPM and XPM increases the phase mismatch and so the FWM efficiency decreases. When the amplifier length increases beyond the L_{op}, the SPM and XPM effects dominate over FWM and hence PSA output power decreases. At the amplifier length of $0.95L_{op}$, the effects of attenuation and SPM and XPM effects compensate for each other, resulting in the maximum PSA output of −4.08 dBm at $0.95L_{op}$.

3.2. PSA gain vs. relative phase between pump signal (ϕ_{rel})

Figure 3 shows the signal power gain G of PSA as a function of signal phase φ_S. The solid line and circle represent the theoretical and simulation results, re-spectively, for $\alpha = 0$ without SPM and SPM effects for amplifier length of L_{op}, and cross (×) represents the simulation results for $\alpha = 0.9$ dB/km with SPM and XPM effects for amplifier length of $0.95L_{op}$. From Figure 3, we observe that PSA gain varies periodically with φ_S and peaks in gain curve occur at the multiple of π , suggesting that signal field is in or out of phase by π resulting in constructive interference at PSA output and is amplified strongly with gain of 2.67 (~ 4.26 dB), while those out of phase by $\pi/2$ go through destructive interference at PSA output causing complete attenuation in both theory and simulation with $\alpha = 0$, thus giving infinite GER ideally. When effects of $\alpha = 0.9$ dB/km with SPM and XPM effects for amplifier length of $0.95L_{op}$ are taken into simulation the gain peak decreases to 1.91 (~ 2.81 dB), while the attenuation in signal is obtained as 0.0066 (~ −21.76 dB) resulting in high GER of 287 (~ 24.57 dB). However, the signal phase at which constructive or destructive interference occurs shifted by $\approx \pi/18$ due to phase shift caused by SPM and XPM effects. This phase-dependent gain forces the phase of signal at PSA output to be nearly 0 or π depending on the initial quadrant in which phase of input signal lies.

3.3. Output signal phase vs. input signal phase (ϕS)

The variation of output signal phase as a function of input signal phase (φ_S) is shown in Figure 4. Output signal phase is forced to a constant value of 0 or π , irrespective of large variation of input signal phase, for $\alpha = 0$ without SPM and XPM effects with amplifier length of L_{op}, in both theory and simulation. When the effects of $\alpha = 0.9$ dB/km with SPM and XPM effects for amplifier length of $0.95L_{op}$ taken into simulation, the output signal phase is nearly constant with small phase shift from 0 or π , while the difference between the two output signal phases is π , suggesting that all amplified signals by PSA has a phase of either 0 or π and are thus useful in phase regeneration of PSK signals.

In brief, we observe that our proposed PSA provides gain of 2.81 dB and forces the output signal to achieve nearly 0 or π phase with high GER of 24.57 dB at amplifier length of $0.95L_{op}$, when effects of α = 0.9 dB/km, SPM and XPM taken into the simulation.

4. Phase regeneration of DPSK signal

In this Section, we discuss the exploitation of PSA in phase regeneration of 100 Gbps single polarization DPSK signal after 1000-km transmission as depicted in Figure 5. The transmission link contains 10 spans of standard single-mode fibre (Length = 100 km, α = 0.2 dB/km, D = 16 ps/nm km), dispersion-compensating fi-bre (Length = 20 km α_{dcf} = 0.5 dB/km, D = −80 ps/nm km) for inline dispersion compensation and optical am-plifier (gain = 30 dB, noise-figure = 5 dB). We have used matlab toolbox Optilux to simulate DPSK transmission (*34*).

Figure 6(a) shows the phasor diagram of degraded DPSK signal after transmission with total phase variation of nearly $5\pi/18$. This phase variation is due to ASE noise of inline optical amplifiers and nonlinear phase noise induced by the transmission fibre. Figure 6(b) shows the same data after phase regeneration by PSA with amplifier length of L_{op} neglecting attenuation, SPM and XPM effects. We obtain 0 or π phase after regeneration by PSA. However, the output phase difference of π is obtained when attenuation α = 0.9 dB/km with SPM & XPM effects are included in PSA with amplifier length of $0.95L_{op}$ as shown in Figure 6(c), thus achieving the near ideal phase regeneration for DPSK signal.

5. Conclusion

In this paper, we proposed and verified a novel scheme of phase-sensitive amplifier (PSA) using cascaded FWM in highly nonlinear fibre. The two phase-conjugate waves generated in first HNLF are used to pump FWM in second HNLF, which results in generation of frequency-shift-free optical phase conjugation. The signal and conjugate waves are combined to obtain constructive or de-structive interference depending upon signal phase and hence the phase-sensitive amplification is obtained. Frequency-shift-free operation helps to amplify the signal without frequency conversion by PSA.

We derived the expression for PSA output signal and PSA gain under lossless condition neglecting the SPM and XPM effects in HNLF. Analytical expression con-firms that PSA gain depends upon signal phase only and thus phase locking between signal and pump is not required. This phase-dependent gain forces signal at the output of PSA to achieve 0 or π phase only, and hence it is useful for PSK regeneration. We have also shown ana-lytically that effects of group velocity, and GVD are mini-mum on signal and conjugate wave propagation and thus on PSA process owing to counter-propagating nature of signal and conjugate waves. Hence, PSA can support a large bandwidth of signal.

We finally investigated the performance of our PSA by simulating PSA under ideal lossless condition (α = 0) without SPM and XPM effects and for α = 0.9 dB/km with SPM and XPM effects in HNLF. Simulation results shown excellent agreement with theoretical value. Fur ther, we simulated the effect of amplifier (PSA) length on output signal and a maximum output signal -4.08 dBm at $0.95L_{op}$ amplifier length is obtained while considering α = 0.9 dBkm^{-1}, SPM, and XPM effects in HNLF. Our PSA scheme offers a gain of 2.81 dB for φ_S = 0 or π and high attenuation for $\varphi_S = \pi/2$, resulting in GER of 24.57 dB and causing degraded DPSK signal to attain π phase difference. A nonlinear phase noise reduction has been simulated and shows a phase regeneration of 100 Gbps DPSK signal transmitted over 1000 km of standard single-mode fibre.

References

(1) Kaminow, I.P.; Li, T.; Willner, A.E. *Optical Fiber Telecommunications Volume VIA: Components and Subsystems*, 6th ed.; Elsevier: New York, 2013.

(2) Umeki, T.; Asobe, M.; Takara, H.; Miyamoto, Y.; Takenouchi, H. Multi-span Transmission Using Phase and Amplitude Regeneration in PPLN-based PSA. *Opt. Express*. **2013,** *21* (15), 18170–18177.

(3) Asobe, M.; Umeki, T.; Tadanaga, O. Phase Sensitive Amplification with Noise Figure below the 3 dB Quantum Limit Using CW Pumped PPLN Waveguide. *Opt. Express*. **2012,** *20* (12), 13164–13172.

(4) Slavik, R. All-optical Phase and Amplitude Regenerator for Next-generation Telecommunications Systems. *Nature Photon.* **2010,** *4*, 690–695.

(5) Das, B.; Abdullah, M.F.L.; Shah, N.S.M. All Optical Signal Restoration for 10G DPSK System. *Ad. Comp. Comm. Engin. Techno.* **2016,** *362*, 545–556.

(6) McKisntrie, C.J.; Radic, S. Phase-sensitive Amplification in a Fiber. *Opt. Express* **2004,** *12*, 4973–4979.

(7) McKinstrie, C.J.; Raymer, M.G.; Radic, S.; Vasilyev, M.V. Quantum Mechanic of Phase-sensitive Amplification in a Fiber. *Opt. Comm.* **2006,** *257*, 146–163.

(8) Tian, Y.; Huang, Y.; Zhang, S.; Prucnal, P.R.; Wang, T. Demonstration of Digital Phase-sensitive Boosting to Extend Signal Reach for Long-haul WDM Systems Using Optical Phase-conjugated Copy. *Opt. Express* **2013,** *21* (4), 5099–5106.

(9) Da Ros, F.; Dalgaard, K.; Lei, L.; Xu, J.; Peucheret, C. QPSK-to-2× BPSK Wavelength and Modulation Format Conversion through Phase-sensitive Four-wave Mixing in a Highly Nonlinear Optical Fiber. *Opt. Express* **2013,** *21* (23), 28743–28750.

(10) Olsson, S.L.I.; Corcoran, B.; Lundstrom, C.; Eriksson, T.A.; Karlsson, M.; Andrekson, P.A. Phase-sensitive Amplified Transmission Links for Improved Sensitivity and Nonlinearity Tolerance. *J. Lightwave Technol.* **2015,** *33*, 710–721.

(11) Olsson, S.L.I.; Lundstrom, C.; Karlsson, M.; Andrekson, P.A. Longhaul (3465 km) Transmission of a 10 GBd QPSK Signal with Low Noise Phase-sensitive In-line Amplification. Presented at the European Conference Exhibition Optical Communication, Cannes, France, 2014.

(12) Neo, R.; Schroder, J.; Paquot, Y.; Choi, D.Y.; Madden, S.; Luther-Davies, B.; Eggleton, B.J. Phase-Sensitive Amplification of Light in a $\chi^{(3)}$ Photonic Chip Using a Dispersion Engineered Chalcogenide Ridge Waveguide. *Opt. Exp.* **2013,** *21*, 7926–7933.

(13) Zhang, Y.; Husko, C.; Schroder, J.; Eggleton, B.J. Record 11 dB Phase-sensitive Amplification in Sub-millimetre Silicon Wave-guides. Presented at the Conference on Lasers and Electro-Optics Pacific Rim, Kyoto, Japan, 2013, 2013, Paper PD1b-3.

(14) Martin, A.; Combrie, S.; Willinger, A.; Eisenstein, G.; de Rossi, A. Interplay of Phase-sensitive Amplification and Cascaded Four-wave Mixing in Dispersion-controlled Waveguides. *Phy. Rev. A* **2016,** *94*, 023817.

(15) Zhang, Y.; Husko, C.; Schröder, J.; Eggleton, B.J. Pulse Evolution and Phase-sensitive Amplification in Silicon Waveguides. *Opt. Lett.* **2014,** *39*, 5329–5332.

(16) Trichili, A.; Zghal, M.; Palmieri, L.; Santagiustina, M. Phase-sensitive Mode Conversion and Equalization in a Few Mode Fiber through Parametric Interactions. *IEEE Phot. J.* **2017,** *9*, 7800710.

(17) Leng, Y.; Richardson, C.J.K.; Goldhar, J. Phase-sensitive Amplification Using Gain Saturation in a Nonlinear Sagnac Interferometer. *Opt. Express* **2008,** *16*, 21446– 21455.

(18) Croussore, K.; Cheolhwan, K.; Guifang, L. All-optical Regeneration of Differential Phase-shift Keying Signals Based on Phase-sensitive Amplification. *Opt. Lett.* **2004,** *29*, 2357–2359.

(19) Croussore, K.; Guifang, L. Phase and Amplitude Regeneration of Differential Phase-shift Keyed Signals Using Phase-sensitive Amplification. *IEEE J. Select. Topics Quant. Elect.* **2008,** *14*, 648–658.

(20) Imajuku, W.; Takada, A.; Yamabayashi, Y. Inline Coherent Optical Amplifier with Noise Figure Lower Than 3 dB Quantum Limit. *Electron. Lett.* **2000,** *36*, 63–64.

(21) Shelby, R.M.; Levenson, M.D.; Bayer, P.W. Guided Acoustic-wave Brillouin-scattering. *Phys. Rev. B* **1984,** *31*, 5244–5252.

(22) Sygletos, S.; Frascella, P.; Rafique, D.; Ellis, A.D. Multi-wavelength Regeneration of Differentially Phase-encoded Signals Using Phase Sensitive Amplification. Presented at International Conference on Photonics in Switching (PS), Ajaccio, 2012.

(23) Weerasuriya, R.; Stylianos, S.; Ibrahim, S.K.; Phelan, R.; OâŁ™Carroll, J.; Kelly, B.; O'Gorman, J.; Ellis, A.D. Generation of Frequency Symmetric Signals from a BPSK Input for Phase Sensitive Amplification. In *Proceedings of OFC 2010 OWT6*, San Diego, CA, USA, 2010.

(24) Anchal, A.; Kumar, P.; Landais, P. Frequency-shift Free Optical Phase Conjugation Using Counter-Propagating Dual Pump Four-wave Mixing in Fiber. *J. Opt.* **2016,** *18*, 116–120.

(25) Anchal, A.; Krishnamurthy, P.K. Phase Conjugation with-out Frequency Shift Using Dual Pumped Bidirectional Fwm in Optical Fibers. In *12th International Conference on Fiber Optics and Photonics, OSA Technical Digest (online)*; Optical Society of America, 2014, Paper S5A.40.

(26) Anchal, A.; Kumar, P.; Landais, P. Mitigation of Nonlinear Effects through Frequency Shift Free Mid-span Spectral Inversion Using Counter-propagating Dual Pumped FWM in Fiber. *J. Opt.* **2016,** *18*, 105703.

(27) Anchal, A.; Krishnamurthy, P.K. Generation of CW Squeezed Light at 1550nm Using Optical Phase Conjugation in Fiber. In *12th International Conference on Fiber Optics and Photonics, OSA Technical Digest (online)*; Optical Society of America, 2014, Paper M4A.27.
(28) Agrawal, G.P. *Nonlinear Fiber Optics*, 4th ed.; Academic Press: New York, 2013.
(29) Okamura, Ya.; Koga, M.; Takada, A. First Demonstration of Phase-sensitive Gain Stabilization by Using Heterodyne Costas Optical Phase-locked Loop. *IEICE Comm. Exp.* **2016,** *5*, 152–157.
(30) HNLF-SPINE ZDW 1540, HNLF Non-Linear Fiber Modules; http://fiber-optic-catalog.ofsoptics.com/item/optical-fibers/highly-nonlinear-fiber-optical-fibers1/ hnlfspine-zdw-1540.
(31) Marconi, J.D.; Boggio, J.M.C.; Callegari, F.A.; Guimaraes, A.; Arradi, R.; Fragnito, H.L. Double Pumped Parametric Amplifier with SBS Suppression by Applying a Strain Distribution to the Fiber. *LEOS, IEEE* **2004,** *2*, 701–702.
(32) Nielsen, L.G.; Jakobsen, D.; Herstrom, S.; Palsdottir, B.; Dasgupta, S.; Richardson, D.; Lundström, C.; Olsson, S.; Andrekson, P.A. *Brillouin Suppressed Highly Nonlinear Fibers*; ECOC, OSA, We.1.F.1, 2012.
(33) Fu, X.; Guo, X.; Shu, C. Raman-enhanced Phase-sensitive Fibre Optical Parametric Amplifier. *Nat. Sci. Reports* **2016,** *6*, 20180.
(34) Optilux matlab toolbox; http://optilux.sourceforge.net/.

Figures

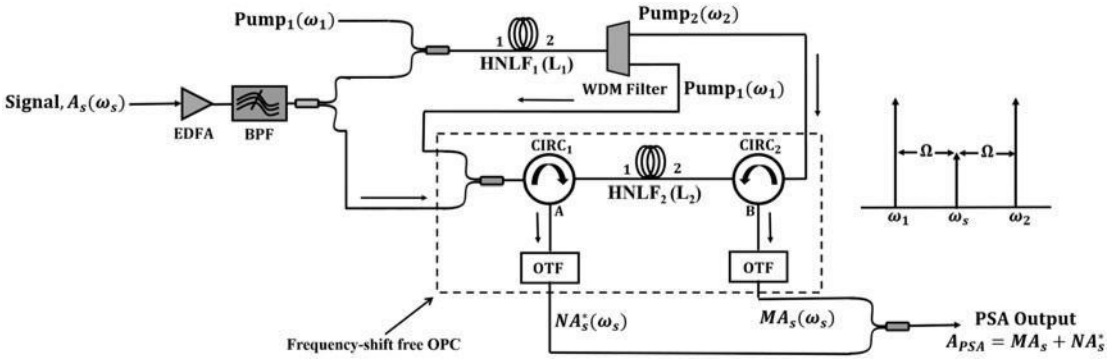

Figure 1. Proposed scheme for phase-sensitive amplifier using cascaded FWM in two HNLF. Two phase-conjugate waves are generated at ω_1 and ω_2 by FWM in HNLF_1, which acts as two counter-propagating pumps for FWM in HNLF_2. The second HNLF constituents the frequency-shift-free OPC as shown in the dotted box. The signal and its conjugate waves are appear at opposite ends of the HNLF_2 with frequency ω_S , which are combined after filtering the pump waves to obtain PSA output signal. $\mathrm{HNLF}_{1,2}$ = highly nonlinear fibre, $\mathrm{CIRC}_{1,2}$ = circulator, DPSK = differential phase-shift keying modulator, OTF = optical tunable filter.

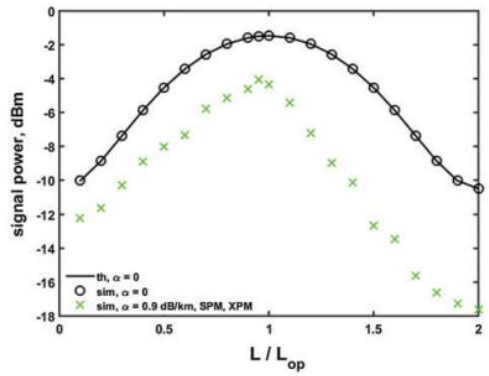

Figure 2. PSA output power as a function of amplifier length. Solid lines and circle (o) shows theoretical and simulation results, respectively, with $\alpha = 0$ without SPM and XPM effects, whereas cross (×) shows the simulation results with $\alpha = 0.9$ dB/km with SPM and XPM effects.

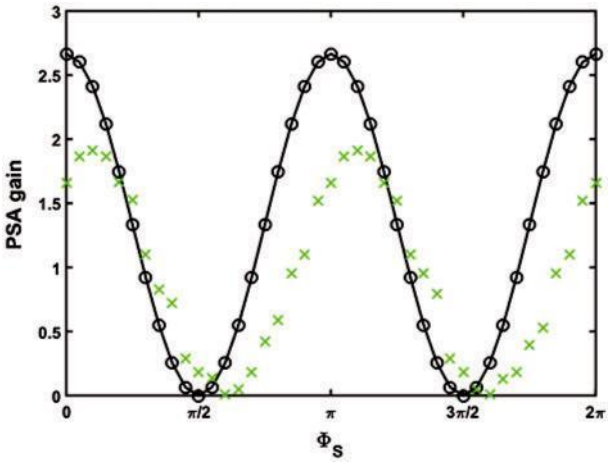

Figure 3. PSA gain as a function of φ_S . Solid lines and circle (o) shows theoretical and simulation results respectively with α = 0 without SPM and XPM effects and amplifier length of L_{op}, whereas cross (×) shows the simulation results with α = 0.9 dB/km with SPM and XPM effects and amplifier length of $0.95L_{op}$.

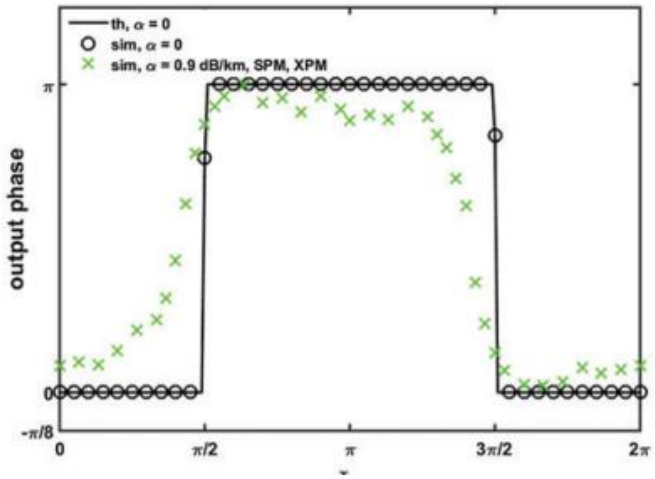

Figure 4. Output signal phase as a function of relative phase between pump signal (φ_{rel}) on signal power gain. Solid lines and circle (o) shows theoretical and simulation results, respectively, with $\alpha = 0$ without SPM and XPM effects and amplifier length of L_{op}, whereas cross (×) shows the simulation results with $\alpha = 0.9$ dB/km with SPM and XPM effects and amplifier length of $0.95L_{op}$.

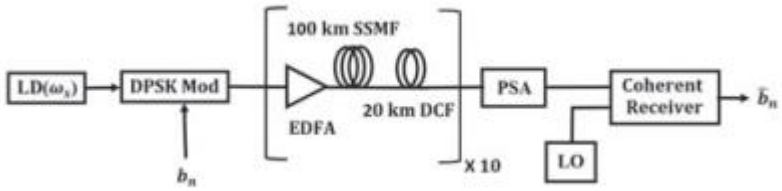

Figure 5. Simulation setup of 100 Gbps single polarization DPSK 1000-km-long transmission network. DCF = dispersion compensating fibre

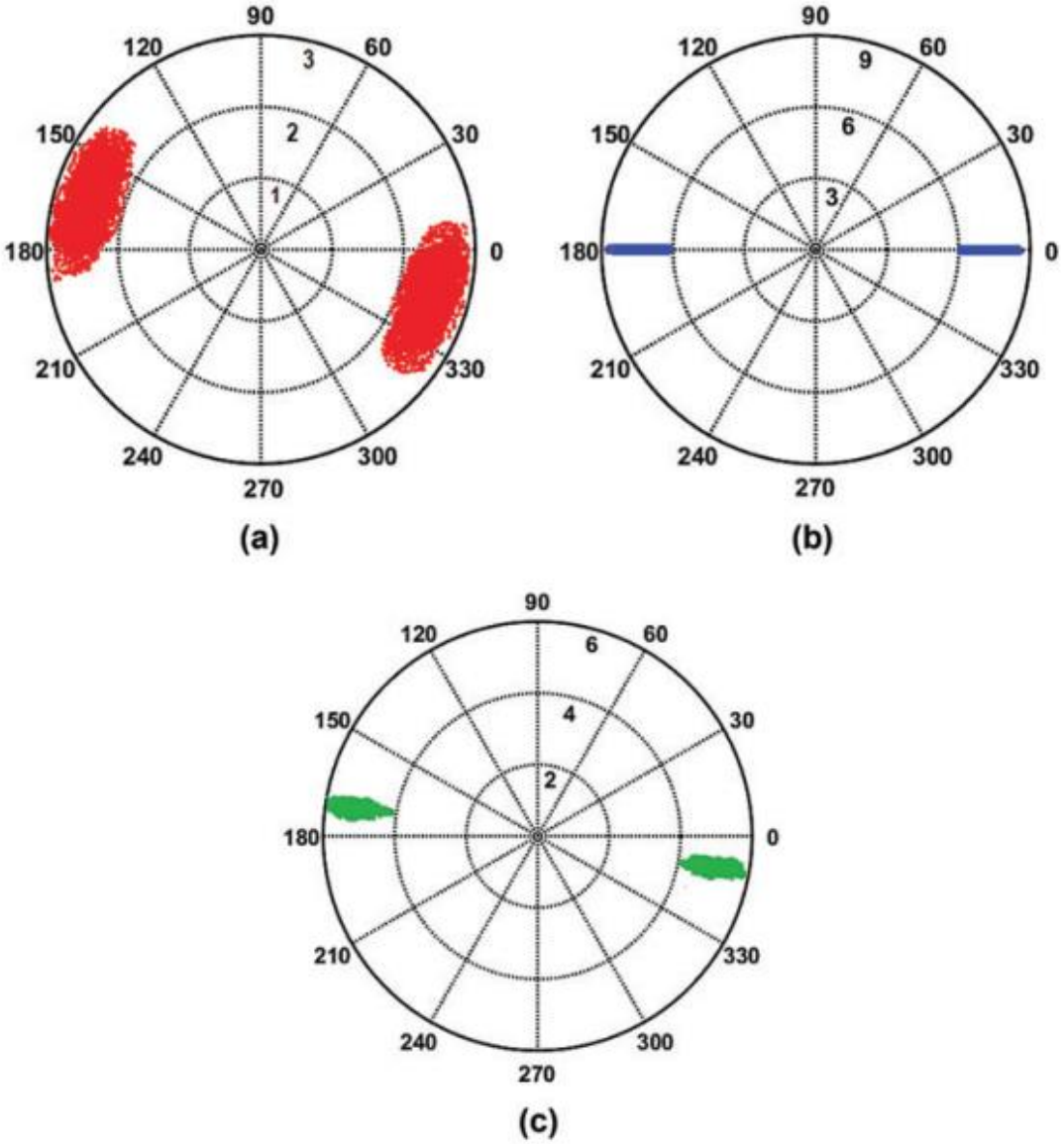

Figure 6. Phasor diagram of DPSK data after 1000-km-long fibre link (a) without PSA implemented, (b) after phase regeneration by PSA under $\alpha = 0$ without SPM & XPM effects, and (c) after phase regeneration by PSA under $\alpha = 0.9$ dB/km with SPM and XPM effects included.